J. Eng. Technol. Sci., Vol. 54, No. 1, 2022, 220114

Multi-Objective Topology Optimization for Curved Arm of Multifunctional Billet Tong Based on Characterization of Working Conditions

Jialiang Liu[1,2,3], Zhaohua Wang[1], Dezhuang Song[1] & Fenghe Wu[1,4,*]

[1]School of Mechanical Engineering, Yanshan University, Qinhuangdao, 066004, China
[2]Mechanics Institute, Shanghai Dianji University, Shanghai, 201306, China
[3]Shanghai Large-scale Casting and Forging Manufacturing Technology Collaborative Innovation Center, Shanghai, 201306, China
[4]Heavy-duty Intelligent Manufacturing Equipment Innovation Center of Hebei Province, Qinhuangdao, 066004, China
*E-mail: risingwu@ysu.edu.cn

Highlights:

- A new multifunctional billet tong was designed for large-scale casting and forging.
- A novel multi-objective topology optimization method for the curved arm of a billet tong is proposed.
- A comprehensive evaluation function was constructed using the compromise programming method.
- A radar chart was employed to determine the weight coefficient of each working condition.
- Using the proposed topology optimization method, the weight of the curved arm could be reduced by 10.77%.

Abstract. A windlass driven heavy duty multifunctional billet tong was designed for large-scale forging and casting to reduce the number of auxiliary material handling devices in manufacturing workshops. To improve its mechanical performance and safety, a novel multi-objective topology optimization method for its curved arm is proposed in this paper. Firstly, the influence of different open angles and working frequencies for the curved arm was simplified to a multi-objective optimization problem. A comprehensive evaluation function was constructed using the compromise programming method, and a mathematical model of multi-objective topology optimization was established. Meanwhile, a radar chart was employed to portray the comparative measures of working conditions, the weight coefficient for each working condition was determined based on the corresponding enclosed areas, combining the stress indices, the displacement indices and the frequency indices of all working conditions. The optimization results showed that the stiffness and strength of the curved arm can be improved while its weight can be reduced by 10.77%, which shows that it is feasible and promising to achieve a lightweight design of the curved arm of a billet tong. The proposed method can be extended to other equipment with complex working conditions.

Received May 18th, 2021, Revised July 29th, 2021, Accepted for publication September 29th, 2021.
 ISSN: 2337-5779,
DOI: 10.5614/j.eng.technol.sci.2022.54.1.14

Keywords: *billet tong; lightweight design; multiple-objective optimization; multiple working conditions; topology optimization.*

1 Introduction

With the advancement of large-scale casting and forging equipment, the components from different fields are increasingly manufactured by large-scale casting and forging owing to various reasons. For example, aircraft structural components, including bulkheads, landing gears and turbine blades, are forged as near-net-shape to improve material utilization and production quality, and to reduce lead/time and cost [1-4]. Heavy-duty components, for instance, the thrust shaft of large marine diesel engines and heavy nuclear power shell rings, are produced by forging due to their large size [5,6]. Recently, the demand for super large-scale forging and casting equipment has been rising in the nuclear power industry due to the shift toward clean energy. The weight of raw materials has even reached up to 500-600 tons [7].

The forging process is a quite complicated manufacturing process, consisting of multiple steps, such as drawing and upsetting [8]. To meet the demands of producing these components, heavy-duty manufacturing equipment, characterized by large sizes, high loads, high inertia and difficult to control, must be systematically investigated [9]. Among others, special auxiliary devices such as lifting tongs and up enders are needed to lift, turn over and transport large-size raw materials. On the one hand, the manufacture of such auxiliary devices is expensive. On the other hand, switching between different auxiliary devices during forging/casting increases the production time. Therefore, the need for multifunctional material handling equipment emerges urgently.

As a lifting device, the lifting tong has attracted increasing attention in recent decades. Its design has evolved from a traditional two-link mechanism to four- and five-link mechanisms; its lifting load for heavy duty tasks can now reach up to 300 tons. However, it is still able to carry out only one or two types of operations (e.g. lifting and/or erecting). In this work, a windlass driven multifunctional billet tong was designed that is capable of performing multiple operations and lifting higher loads. Its maximum lifting load is 550 tons, and its net weight reaches up to 104.59 tons. The maximum lifting load and net weight have a large effect on the performance of billet tongs collectively. These features determine the behavior of heavy-duty manufacturing equipment [9]. It is difficult for billet tongs as typical heavy-duty manufacturing equipment to implement operations stably, accurately, smoothly and safely with too high load and high inertia. Normally, the design of a billet tong relies heavily on the personal skills of experienced designers. Finite element analysis (FEA) tools have been employed to iteratively evaluate design alternatives with different assigned safety

factors [10]. Although this approach allows weight savings to some extent, it still cannot make full use of the material due to the adoption of conservative safety factors. Meanwhile, the iterative evaluation work is tedious and time-consuming.

Benefitting from the development of finite element technology and personal computers, topology optimization as a systematic way of achieving lightweight designs has been widely used in different industrial fields [11-14]. In this work, topology optimization was firstly applied to achieve a lightweight billet tong design. By adjusting the open angle, the billet tong is able to grab ingots with varying shapes and sizes. Its load transfer path varies accordingly. Hence, topology optimization of the billet tong is a typical topology optimization problem of a continuum structure with multiple loads or working conditions [15]. Since this problem exists in many practical applications, it has been investigated by using the homogenization method [16-18], the level-set method [19], the Solid Isotropic Material with Penalization (SIMP) method [20-25], the Rational Approximation of Material Properties (RAMP) method [26], the Independent Continuous and Mapping (ICM) method [27,28], the Evolutionary Structural Optimization (ESO) method [29], evolutionary algorithms (EA) [30,31] and a hybrid approach [32]. SIMP is popularly adopted, among others because of its theoretical simplicity and ease of implementation [11,33]. Moreover, its physical rationality when certain conditions are satisfied has been proved [34] and it is supported by many commercial CAE tools, for example, Ansys, Abaqus and Hyperworks, which make it easily accessible for users. The SIMP method was also adopted in the present study.

Originally, topology optimization of a continuum structure was expressed as a type of integer programming problem with design variables that switch between 0 and 1, which makes the optimization problem ill-posed. SIMP innovatively introduced the relative density of the material, which continuously varies from 0 to 1, thus transforming discrete optimization into continuous optimization [35]. It is assumed that a nonlinear relationship exists between the material's macroscopic elastic modulus and its density. A penalty factor is adopted to push the cells with intermediate densities close to 0 or 1, which correspond to a 'void' or a 'solid' design, respectively. With the volume constraint, a topology optimization problem with maximum stiffness/minimum compliance as objective is established. To eliminate the checkerboard and mesh dependence issues that are normally involved in SIMP, additional numerical measures must be conducted, for example, the method of moving asymptotes (MMA) [36]. In order to implement SIMP for topology optimization of billet tongs, the following issues have to be addressed:

1. **Ill-load problem**. The load transfer path of the structure is different under different loading conditions. During the iterations of optimization, the load

transfer path supporting smaller loads may disappear. This is a common issue in multiple loading cases and is designated as load ill-posedness or ill load cases [23,28]. As noted above, billet tongs must be able to grab ingots with various shapes, sizes and weights, so the ill-load problem must be taken into consideration in the topology optimization method.

2. **Characterization of multiple working conditions**. McKee & Porter [37] explain that the optimization of lifting hangers based on topology optimization should also take working conditions that do not occur very often into consideration. Generally, this issue is addressed by choosing an appropriate safety factor. However, choosing an appropriate safety factor is a challenge. In practice, relatively conservative safety factors are selected. During casting/forging, the ingots undergo drawing and upsetting operations that change their size. The billet tong has to be able to adjust its open angle to enable the accomplishment of each operation. Most importantly, the frequency is quite different for each of the operations. Since these operations are performed in a high temperature environment, operation with a high frequency cause more fatigue damage to the billet tong from the high temperatures it is exposed to. Thus, not only multiple loads but also the frequency of loads needs to be known to characterize the diverse working conditions in a more comprehensive way.
3. **Weight determination method**. When the stiffness of the structure is set as the optimization objective, the goal of optimization is to find the maximum stiffness under a certain load. With multiple loads, the goal becomes to find a compromise overall stiffness. Hence, topology optimization of a continuum structure with multiple loads is modeled as a multiple objective optimization problem [20]. In order to obtain a determinate solution rather than the whole Pareto front, various weighted sum methods are widely used to convert the multiple objective optimization into single objective optimization [38]. As the weighted sum methods and the weight values influence the performance of the optimization results, both must be carefully selected in accordance with the working conditions [39].

In view of the aforementioned issues, a novel multi-objective topology optimization method for the curved arm of a multifunctional billet tong is proposed in this paper. As described above, SIMP was selected as the density-stiffness interpolation scheme for the proposed method. Inspired by [27,28], each load condition is converted into strain energy to evaluate the load effect on the overall stiffness to deal with the ill-load problem. Meanwhile, the working conditions of the billet tong are characterized in terms of stress, displacement, and frequency simultaneously. To be able to visually and quantitatively illustrate each working condition, a radar chart was employed to portray these three comparative measures. Meanwhile, the compromise programming method was chosen as the weighted sum method to convert multi-objective optimization into

single objective optimization. Based on the radar chart, the weight for each working condition is determined by the ratio of the area of the corresponding enclosed triangle to the sum of the triangular areas for all working conditions. Consequently, the weights can reflect the contribution of each aspect of the working conditions in an objective manner. The optimization result showed that the proposed method is feasible and promising to achieve a lightweight design of the curved arm of a billet tong.

The rest of this paper is organized as follows. In Section 2, related works that deal with ill-load cases and weight determination for multi-objective topology optimization are reviewed. The design of the multifunctional billet tong and its lightweight requirement are introduced in Section 3. Section 4 discusses the proposed SIMP-based topology optimization formulation and the weight determination method using a radar chart. The optimization results and discussions are provided in Section 5 and the conclusions can be found in Section 6.

2 Related Work

As the proposed method uses the compromise programming method to convert multi-objective topology optimization to single objective optimization for multiple working conditions, related works that deal with ill-load cases and weighted sum methods for multi-objective topology optimization are reviewed.

2.1 Dealing with Ill-load Cases for Multi-Objective Topology Optimization

To perform topology optimization for structures with stress constraints under multiple loading cases, Sui, *et al.* [27,28] proposed the independent continuum map method to convert the stress constraints to strain energy constraints to reduce the computational load. Benefitting from adopting strain energy as constraints, even though the strain energy induced by a small load is low, its effect on the structure can still be well reflected. Accordingly, an optimization model can be established to minimize structure weight with minimum allowable structure strain energy constraints. Similarly Luo, *et al.* [26] also applied strain energy rather than load to express the effect of load on structure stiffness. Cai, *et al.* [23] applied q-norm to create fractional-norm weighted mean structural compliance as objective function. By controlling the value of q, the ill-load problem can be mitigated. Later, this method was extended for bi-modulus materials [40,41] and multiphase bi-modulus materials [42]. Increasing the small loads is a straightforward way of dealing with ill-load cases, but the effects induced by increments of small loads and large loads are quite different. Hence, Li, *et al.* [24] introduced the amplification coefficient (AC) to amplify small loads to deal with ill-load cases.

The AC value is defined as the ratio of the change of structural properties caused by a load increment to the original structural properties without load increment. Since strain energy is well able to reflect the effect of load on structural stiffness, it was adopted in the proposed method to deal with ill-load cases.

2.2 Weight Determination Methods for Multi-Objective Topology Optimization

To be able to get a determinate optimal solution, various weighted sum methods, such as the compromise programming method [20], the linear weighting method [38], the weight-square method [24] and the weight-norm method [23], can be applied to convert the multi-objective optimization problem into a single objective optimization problem. No matter which method is applied, the calculation of the weight factor for each objective is critical, since the weights have a significant effect on the final optimization result. Sui, *et al.* [27,28] converted the stress constraints to strain energy constraints. Accordingly, the effect of multiple loading cases on the structure can be weighted by the corresponding structure strain energy as well. Luo, *et al.* [26] investigated a multi-objective topology optimization scheme for compliant mechanism design. In the proposed approach, maximizing mutual strain energy and minimizing strain energy are selected as conflicting objectives. The compromise programming method is employed to convert multiple objective optimization to single objective optimization. As for the weighting method, the weighting coefficient is determined by maximization of the mutual energy and minimization of the mean compliance.

Wu, *et al.* [43] applied the Analytic Hierarchy Process (AHP) method to calculate the topology optimization weights for a diesel engine cylinder block with the compromise programming method. Li & Wang [44] applied the α-method to calculate the weights for each objective using a linear weighting method. Luo, *et al.* [20] proposed an expert evaluation method based on grey system theory to calculate the weights for multi-objective problem. In order to reduce the subjective influence of the designer and increase the robustness of the optimization results, a closed interval is provided by experts rather than a point value for each objective. The final weight for each objective is a synthesis of all experts' evaluations. They also extended this method to solve multi-objective topological optimization of static and dynamic structures [45]. The optimization problem is modeled as a goal programming problem. To obtain more accurate aspiration levels associated with each objective, fuzzy set theory is applied. Li, *et al.* [21] developed a normalized exponential weighted criterion method to search the entire Pareto frontier for extended optimality to solve multi-topology optimization problems. They provided a weight evaluation method based on fuzzy multiple attribute group decision-making theory to guarantee an optimal

design at an acceptable level. Suresh *et al.* [46] describe an adaptive weighting strategy in which the weight calculation method is adjusted among a linear function, a quadratic function, and an exponential function based on constraint violations to obtain better optimization results for different problems.

Li, *et al.* [24] proposed a load case severity degree (LCSD) based weight value calculation method for topology optimization with multiple loading cases. The LCSD is defined as the ratio between the single condition optimization result under each loading case and the critical optimization result under the corresponding loading case to portray the threat degree of the optimized design variables of each loading case to successfully achieve the optimal goal. The ratios between the products of LCSD and AC for different loading cases are used to determine the corresponding weight values. The proposed method was compared with AHP, the tolerance method, the empirical method, and the α method when a linear weighting method, a weight-square method, a weight-norm method, and a compromise programming method respectively are employed as weighted sum method. The comparison results showed that the proposed method is not much affected by the weighted sum method used and can deal with ill-load cases. Qiao, *et al.* [22] developed a hybrid weight determination method that combines the AHP-based method and the orthogonal test-based method to achieve a balance between subjective judgement and objective calculation. The weight value is calculated for each load case, using the AHP-based method and the orthogonal test-based method respectively. Then the ratio between their sum and the sum of the weight values for all loadings is selected as the final weight value for this loading case. Ismail, *et al.* [47] investigated the topology optimization of a bicycle crank with multiple load cases. Uphill angles of 10°, 20° and 30° were selected to reflect the variation of the working conditions. For each working condition, the weight for each uphill angle value was determined manually based on the dominance of each angle value in the working condition.

In summary, the current weight determination methods do not consider load frequency as part of the working conditions. Therefore, a more comprehensive working condition characterization method is needed. Moreover, a new weight determination method that can deal with complex working conditions is needed as well.

3 Lightweight Design Requirement of Billet Tong

According to the industrial partners' requirements, a windlass driven multifunctional billet tong was designed, as shown in Figure 1. Its specifications are listed in Table 1. The upper end of the billet tong is connected to an overhead crane by a hinge pin. The windlass is fixed on a platform that is used to connect the hinge pin with the main shaft. The fixed pulley block mounted on the main

shaft connects with the movable pulley block, which is installed on the beam by the wire ropes of the windlass.

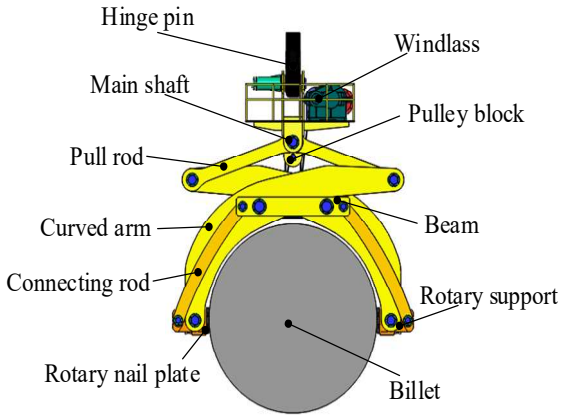

Figure 1 Multifunctional billet tong.

Table 1 Specifications of billet tong.

Technical Parameters	Value
Length of workpiece	2~6 m
Size of billet tong	8.6*2.2*11.5 (L*W*H, m)
Maximum lifting load	550 tons
Net weight	104. 95 tons
Working temperature	0~1200 ℃
Workpiece surface indentation	≤ 50 mm
Maximum displacement	30 mm
Operating life	≥ 30 years

By moving the beam up and down along the vertical direction, the curved arm, the pull rod and the connecting rod are collectively driven to make the billet tong open and close. Two parallelogram mechanisms made up by the connecting rods, curved arm, rotary support and beam ensure that the bilateral jaws are always in parallel. As a result, ingots can be transported smoothly. The bilateral jaw consists of a rotary support and a rotary nail plate. The rotary nail plate can rotate around the axis of the rotating support by the weight of the ingots to perform turning over and erecting operations. The maximum allowable indentation of the nail plate into the workpiece is 30 mm, which ensures that the surface quality of the workpiece remains acceptable. The rotary nail plate is made of heat resistant steel FCH1, which has good oxidation resistance at 1200 °C. The other components are made of high strength steel Q690. Various operations performed with the billet tong are demonstrated in Figure 2.

(a) Erecting (b) Lifting up (c) Turn over (d) Transport

Figure 2 Demonstration of various operations performed by the billet tong.

3.1 Load Analysis

The combined weight of the billet tong and the ingot is borne by 8 wire ropes. The number of wire ropes increases along with the increased weight of the billet tong. In order to improve the performance of the billet tong and to ensure a safer working environment, the billet tong should be designed as light as possible. The quantity and weight of each component of the billet tong are listed in Table 2. The curved arm accounts for 55.55% of the overall weight. Therefore, it was selected for structural optimization.

Table 2 Specifications of components.

Component	Quantity	Weight (tons)	Percentage (%)
Pull rod	4	2.48	9.48
Beam	2	2.61	4.99
Curved arm	2	29.05	55.55
Connecting rod	4	1.68	6.43
Others	15	24.63	23.55

As described above, the billet tong can grab ingots of various shapes, sizes and weights by adjusting the open angle/distance. The load transfer path varies accordingly. In order to improve the optimization efficiency without loss of generality, the open distance was discretized into 2 m, 3 m, 4 m, 5 m and 6 m, as shown in Figure 3. Taking the open distance of 6 m as an example, a schematic diagram of the the billet tong mechanism is shown in Figure 4. The loads of the left curved arm $\overline{CEI}$ include gravity G, billet weight $G_g^{'}$, the pulling force from the pull rod F_C, and the restraint load from the pin (point E).

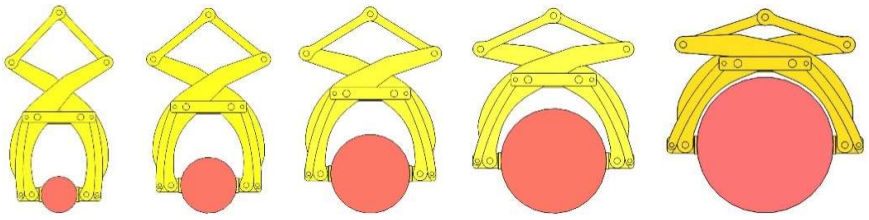

Figure 3 Discretization of open distance: (a) 2 m, (b) 3 m, (c) 4 m, (d) 5 m, and (e) 6 m.

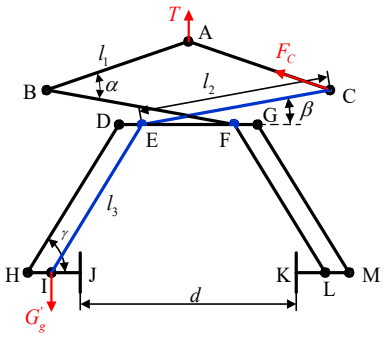

Figure 4 Schematic diagram of the mechanism of the billet tong.

Therefore, the gravity G_g' for one side can be calculated by Eq. (1):

$$G_g' = \frac{G_g}{2} \tag{1}$$

where, G_g is the weight of the billet.

As the pull rod is a typical two-force bar, the force direction is along the axis of the pull rod when the billet tong is in equilibrium state. Therefore, the force of the right pull rod applied to the curved arm is expressed by Eq. (2):

$$F_C = \frac{\mathrm{T}}{2\sin(\alpha - \beta)} \tag{2}$$

where F_C is the force the right pull rod applies to the curved arm, and T is the overall weight of the billet tong and billet. The angles α, β, γ are defined as

shown in Figure 4 and their values for discretized open distances are listed in Table 3.

Table 3 Angles for discretized open distances.

Open distance (m)	α (°)	β (°)	γ (°)
2	84.63	38.30	85.87
3	70.56	31.55	79.12
4	56.44	24.64	72.21
5	42.27	17.44	65.01
6	28.38	9.80	57.37

3.2 Finite Element Analysis

The material properties of the curved arm are shown in Table 4. The applied forces, including gravity, steel billet weight, and pulling force from the pull rod, are shown in Figure 5. The freedom constraints are applied at two holes (hole E and hole I), where T_x and T_y mean that the displacement is limited in the x and y directions, and R_x and R_z mean that the rotation angle is limited in the x and z directions.

Table 4 Material properties of curved arm (Q690).

Elastic modulus (MPa)	Passion's ratio	Density (kg/m^3)	Yield strength (MPa)
2.14e5	0.29	7850	690

FEA was carried out for the curved arm with different open distances in Ansys 18.0. The element type was set to tetrahedral element and the element division method was set to automatic. To ensure the accuracy of the FEA results, the meshing convergence was first verified by calculating the maximum displacement and stress with different element sizes with the open distance at 6 m. The variation trends with 44~60 mm element size are shown in Figure 6. As shown in Figure 6(a), the maximum displacement remains the same when the element size is smaller than 50 mm. The smaller the element size, the greater the local stress value in Figure 6(b). The main reason is that an element size that is too small easily induces stress concentration. As a result, the convergence solution can be obtained when the element size is 50 mm, as shown in Figure 7. The final numbers of elements and nodes were 270,452 and 458,269 respectively.

Since the speed of movement of the billet tong during working is quite low, only static characteristics were considered in this study. The displacement and stress distribution of the curved arm were calculated for different open distances. As strain energy was used to attribute the effect of different loads on the structure, this was calculated as well. All results are listed in Table 5.

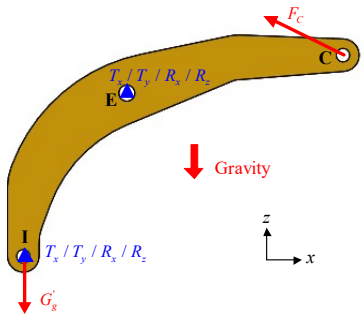

Figure 5 The loads and boundary conditions of the curved arm.

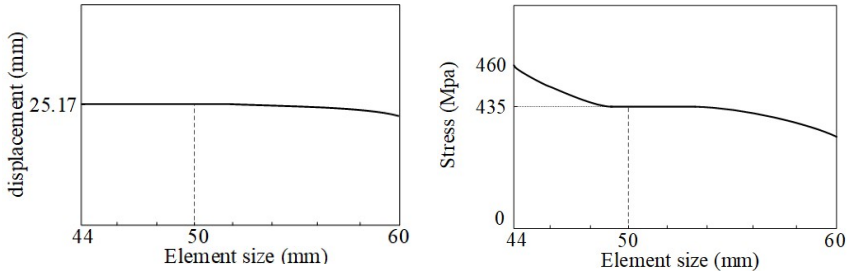

Figure 6 Verification of meshing convergence: (a) maximum displacement; (b) maximum stress.

Figure 7 The finite element model (FEM) of the curved arm.

It was found that the maximum stress of the curved arm, 463.63 MPa, was smaller than the material yield strength of 690 MPa, and the maximum displacement of 29.51 mm was smaller than the allowable maximum displacement of 30 mm. The maximum stress occurred at the position of the middle hole due to stress concentration when the open distance was 5 m, as shown in Figure 8. The stress of the other regions ranged from 50 MPa to 150 MPa. Apparently, the curved arm has a large optimization space for material savings.

Table 5 FEA results.

Open distance (m)	Max displacement (mm)	Max stress (MPa)	Strain energy (N*mm)
2	26.84	386.34	4488.9
3	28.61	418.48	4921.0
4	29.51	447.76	5526.9
5	28.87	463.63	5735.9
6	25.17	435.25	5023.1

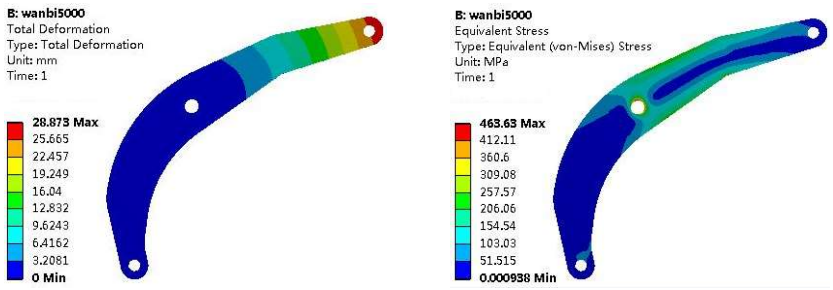

(a) (b)

Figure 8 The FEA results for an open distance of 5 m: (a) displacement distribution, and (b) stress distribution.

4 Multi-Objective Topology Optimization Method

4.1 Optimization Formulation

In the proposed topology optimization method enabled by SIMP, the relative density is selected as the design variable, as expressed by Eq. (3):

$$\begin{cases} E(\rho) = \rho^p E \\ 0 < \rho_{\min} \le \rho \le 1 \end{cases} \tag{3}$$

where, ρ is the material relative density, $\rho_{\min}$ is the material minimum relative density, E is the material elastic modulus, and p is the penalty factor with $p > 1$.

The compliance was selected as the optimization objective. As introduced before, there are many methods to convert multiple objective optimization into single objective optimization. The compromise programming method was adopted in this work because it can get a group of better relative optimal solutions by calculating the sensitivity of all objective functions against the design variable, and by balancing the objectives between each other, even for a nonconvex

optimization problem [48]. The objective function for compliance obtained by the compromise programming method is calculated by Eq. (4):

$$\min_{\rho} C(\rho) = \left\{ \sum_{i=1}^{m} w_i^q \left[\frac{C_i(\rho) - C_i^{\min}}{C_i^{\max} - C_i^{\min}} \right]^q \right\}^{\frac{1}{q}} \tag{4}$$

where m is the total number of working conditions, w_i is the weight coefficient of the i-th working condition, q is the penalty coefficient ($q \geq 2$), $C_i(\rho)$ is the compliant objective function of the i-th working condition, $C_i(\rho) = \mathbf{u}^{\mathrm{T}}\mathbf{K}\mathbf{u}$, $\mathbf{u}$ is the displacement vector of each node of the finite element; $\mathbf{K}$ is the overall stiffness matrix of the structure; $C_i^{\max}$ and $C_i^{\min}$ are the maximum and minimum compliant objective functions of the i-th working condition, respectively.

With the density constrain and volume constraint, the multi-objective topology optimization of the curved arm was established as shown in Eq. (5):

$$\begin{cases} \text{Find} \quad \rho = (\rho_1, \cdots, \rho_n) \\ \min \quad C(\rho) = \left\{ \sum_{i=1}^{m} w_i^q \left[\dfrac{C_i(\rho) - C_i^{\min}}{C_i^{\max} - C_i^{\min}} \right]^q \right\}^{\frac{1}{q}} \\ \text{Subject to} \quad \mathbf{K}(\rho)\mathbf{u} = \mathbf{P} \\ \qquad\qquad c(\rho) = \mathbf{u}^T\mathbf{K}\mathbf{u} = \sum_{e=1}^{n} (\rho_e)^p \mathbf{u}_e^T \mathbf{K}_e \mathbf{u}_e \\ \qquad\qquad V(\rho) \leq 0.7 \cdot V_0 \\ \qquad\qquad 0 < \rho_{\min} \leq \rho_i \leq 1 \end{cases} \tag{5}$$

where, $\mathbf{u}_e$ is the displacement vector of the e-th element; $\mathbf{K}_e$ is the stiffness matrix of the e-th element; $\mathbf{P}$ is the load vector; $V(\rho)$ is the optimized volume; V_0 is the volume before optimization. As the values of w_i affect the final topology optimization results, it must be determined based on multiple working conditions in an objective way.

4.2 Characterization of Working Conditions

According to Miner's law, a material will be damaged gradually when it works under a certain stress for a period of time. This fatigue process can be accelerated by a high temperature environment. The billet tong has to perform various operations in a high temperature environment during forging and casting.

Therefore, not only the magnitude and location of the load but also the frequency of the operations with different loads has to be known to characterize the working conditions of the billet tong in a more comprehensive way. Accordingly, the structural strength and stiffness under different loads and the corresponding frequency are used as features of the working conditions. Based on statistics provided by the industrial partner, the frequencies for different open distances of the billet tong are listed in Table 6.

Table 6 Frequency of working conditions.

Open distance (m)	2	3	4	5	6
Annual frequency	120	100	75	60	40

In order to accurately reflect the influence of these features, the stress, displacement, and frequency of the curved arm under different working conditions were normalized and defined as stress index I_σ, displacement index I_d, and frequency index I_f, respectively by Eq. (6):

$$\begin{cases} I_\sigma(i) = \sigma_i / \sigma_{\mathrm{T}} \\ I_d(i) = d_i / d_{\mathrm{T}} \\ I_f(i) = f_i / f_{\mathrm{sum}} \end{cases} \tag{6}$$

where, σ_i, d_i, f_i are the maximum stress, displacement, and frequency under the *i*-th working condition respectively; $\sigma_{\mathrm{T}}, d_{\mathrm{T}}, f_{\mathrm{sum}}$ is the stress threshold, displacement threshold and the sum of all frequencies, respectively. In this paper, the material yield strength was chosen as the structural stress threshold and the displacement threshold was 30 mm according to the design requirement. The indices values for five working conditions of the billet tong are listed in Table 7.

Table 7 Characteristic indices of working conditions.

Open distance (m)	**2**	**3**	**4**	**5**	**6**
Stress index	0.560	0.606	0.649	0.672	0.631
Displacement index	0.895	0.954	0.984	0.962	0.839
Frequency index	0.304	0.253	0.190	0.839	0.101

4.3 Weight Determination Method Using Radar Chart

To be able visualize the characteristic indices of the working conditions, a radar chart was applied, because it can clearly and accurately reflect the relative positions of all comparative measures based on their values [49,50]. A radar chart generated using the data from Table 7 is shown in Figure 9.

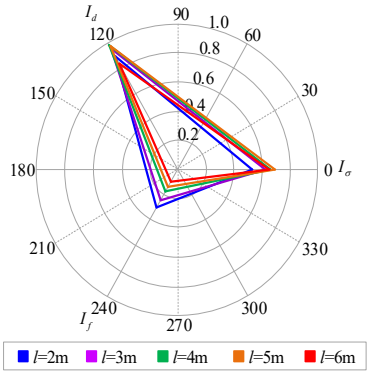

Figure 9 Radar chart of working condition.

Based on the radar chart, the contribution of each working condition for the overall stiffness was determined by the ratio between the area of the corresponding enclosed triangle and the sum of triangular areas for all working conditions, as represented by Eq. (7). Most importantly, this ratio can be used as the weight factor for each working condition.

$$w_i = A_i / \sum_{i=1}^{m} A_i \tag{7}$$

where A_i is the area of the enclosed triangle of the i-th working condition.

The area of the enclosed triangle of each working condition and the corresponding weight factor are listed in Table 8. It is noted that the contribution of open distance 3 m was the largest. The open distance of 5 m, which had the maximum stress, actually did not contribute too much. Therefore, the proposed weight determination method better reflects the importance of each working condition in an objective way.

Table 8 Summary of physical parameters.

Open distance (m)	2	3	4	5	6
A_i	0.099	0.105	0.104	0.099	0.074
w_i	0.206	0.219	0.216	0.205	0.154

5 Results and Discussions

The topology optimization of the curved arm first has to identify design regions and non-design regions, as shown in Figure 10. The upper, middle and lower round holes of the curved arm are non-design areas (marked in red). In order to prevent the curved arm and the pulley block from interfering with each other

during working, the red dotted frame area in Figure 10 between the upper layer and the lower layer cannot add any material. To fully exploit the load-bearing capacity of the material, the design regions were identified as shown in the Figure 10.

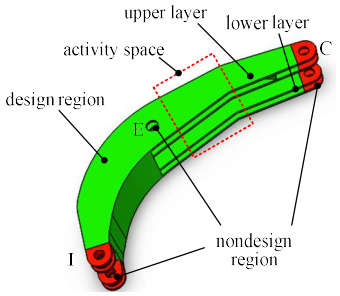

Figure 10 Identification of design regions of the curved arm.

The topology optimization result generated by the proposed method in OptiStruct 14.0 is shown in Figure 11. The regions marked from blue to red indicate that the material becomes increasingly more important. According to the result, the material between the upper and middle holes must be kept, while some of the material between the lower and the middle holes can be removed. To ensure the stability of the curved arm, the regions between the middle hole and the lower hole were designed as a box-type structure. The arrangement of the internal ribs, also called the load flow pattern, was done following the topology optimization result and lightweight holes were added in some areas, as shown in Figure 12. Through optimization, the weight of the curved arm was reduced to 25.92 tons, which means 10.77% of material savings were achieved. The lightweight result is remarkable.

FEA was carried out again for the optimized curved arm with different working conditions to verify the proposed topology optimization method. The same element type and element meshing method were applied. The meshing convergence was verified, and the result showed that the element size should be set to 35 mm, as shown in Figure 13. The number of elements and nodes was 726,893 and 1,153,259 respectively.

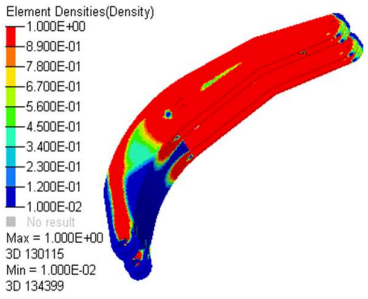

Figure 11 Topology optimization result.

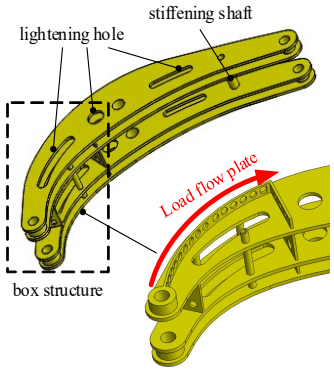

Figure 12 Optimized design of the curved arm.

Figure 13 The finite element model (FEM) of the new curved arm.

Comparisons between the original design and the optimal design were made in terms of maximum displacement and maximum stress, as shown in Figures 14 and 15, respectively. It can be seen that the maximum displacement was reduced by about 15%, and the maximum stress was reduced by approximately 10%.

Taking the working condition with an open distance of 5 m as an example again, the maximum displacement was reduced from 28.87 mm to 24.25 mm, and the maximum stress was reduced from 463.63 MPa to 408.27 MPa, which still

occurred at the middle hole. The stress distributed in the other regions ranged from 90 MPa to 180 MPa in a more uniform manner. The FEA details are shown in Figure 16 and listed in Table 9.

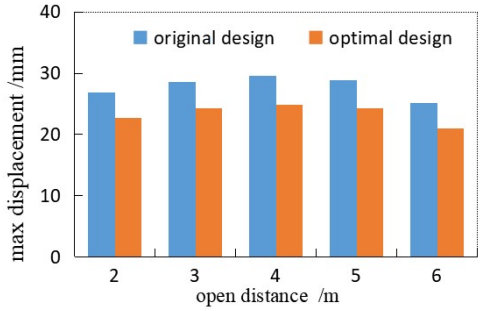

Figure 14 Comparison of the maximum displacement.

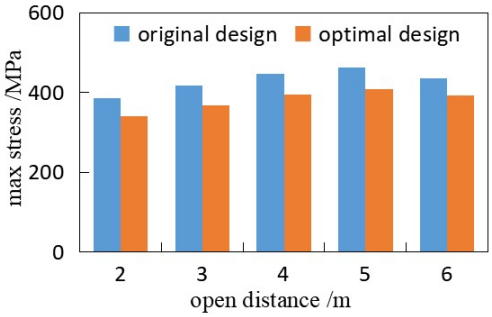

Figure 15 Comparison of the maximum stress.

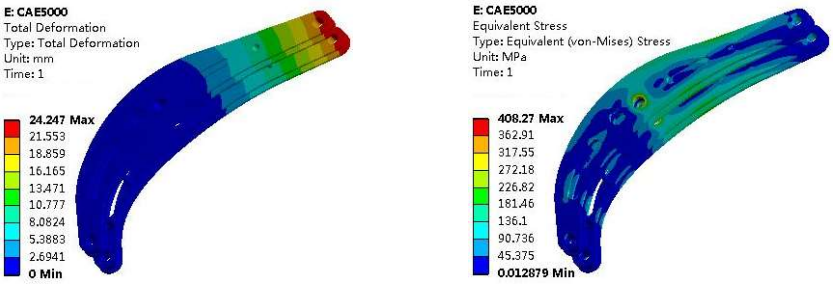

(a) (b)

Figure 16 FEA results of the optimal design: (a) displacement distribution, and (b) stress distribution.

Table 9 Comparison for open distance 5 m.

	Weight (tons)	Maximum displacement (mm)	Maximum stress (MPa)
Original design	29.05	28.87	463.63
Optimal design	25.92	24.25	408.27
Deviation	-3.13	-4.62	-55.36
Percentage	-10.77%	-16%	-11.94%

6 Conclusions

In this paper, a novel multi-objective topology optimization method for the curved arm of a multifunctional billet tong is proposed. The proposed method can be extended for the lightweight design of many other equipment/components that run in multiple working conditions, such as cranes, automobile frames, and machine tools. The main contributions of this paper can be summarized as follows:

1. A heavy-duty multifunctional billet tong was designed for large-scale forging and casting. In order to reduce the number of currently needed auxiliary devices and to increase manufacturing efficiency, a windlass driven multifunctional billet tong was designed to perform various operations, such as erecting, lifting, turning over, and transporting. Its maximum lift load can reach up to 550 tons.
2. Comprehensive characterization of working conditions. Through analyzing the working environment of the billet tong, it was found that the working condition frequency has a remarkable effect on the operating life of the billet tong. Therefore, compared with current methods, which only consider the magnitude and location of loads, working condition frequency was added to characterize the working conditions of the billet tong more comprehensively.
3. Objective weight determination method. A radar chart was adopted to portray the working conditions of the billet tong. Based on the radar chart, the ratio between the area of the enclosed triangle for each working condition and the sum of the triangular areas for all working conditions was employed as the corresponding weight factor. Since the weight factor can reflect the contribution of each working condition in a more comprehensive way, this is a more objective method. This method can be extended to other applications that involve complex working conditions.
4. Promising material saving. By using the proposed topology optimization method, the weight of the curved arm could be reduced by 10.77%.

Acknowledgement

The authors highly appreciate the valuable comments from the editor and all reviewers. This work was supported by the Chinese National Key Research and

Development Program (2016YFC0802900), the Key Natural Science Projects of Hebei Provincial Department of Education (ZD2020156), and the open project of the Heavy-duty Intelligent Manufacturing Equipment Innovation Center of Hebei Province (201906).

References

[1] Calvert, E., Wynne, B., Weston, N., Tudball, A. & Jackson, M., *Thermomechanical Processing of a High Strength Metastable Beta Titanium Alloy Powder, Consolidated Using the Low-cost FAST-Forge Process*, Journal of Materials Processing Technology, **254**, pp. 158-170, 2018.

[2] Luo, S., Zhu, D., Qian, D., Hua, L., Yan, S. & Zhang, J., *Effects of Friction Model on Forging Process of Ti-6Al-4V Turbine Blade Considering the Influence of Sliding Velocity*, The International Journal of Advanced Manufacturing Technology, **82**(9-12), pp. 1993-2002, 2016.

[3] Zhang, D-W. &Yang, H., *Preform Design for Large-scale Bulkhead of TA15 Titanium Alloy based on Local Loading Features*, The International Journal of Advanced Manufacturing Technology, **67**(9-12), pp. 2551-2562, 2013.

[4] Marini, D., Cunningham, D. & Corney, J.R., *Near Net Shape Manufacturing of Metal: A Review of Approaches and Their Evolutions*, Proceedings of the Institution of Mechanical Engineers, Part B: Journal of Engineering Manufacture, **232**(4), pp. 650-669, 2017.

[5] Kwon, I-K. &Park, H-S., *Design of Die Forging Process of Thrust Shaft for Large Marine Diesel Engine Using Floating Die Concept*, International Journal of Precision Engineering and Manufacturing, **12**(3), pp. 527-535, 2011.

[6] Fu, X., Liu, B. & Zhang, Y., *Measurement Technology of the Hot-state Size for Heavy Shell Ring Forging*, The International Journal of Advanced Manufacturing Technology, **65**(1-4), pp. 543-548, 2012.

[7] Greger, M., *Forging*, Technical University of Ostrava, 2014.

[8] Donth, B., Blaes, N., Diwo, A. & Böttcher, D., *Large-Scale Manufacture of Nickel Alloy Turbine Rotor Forgings for A-USC Power Plants*, Transactions of the Indian National Academy of Engineering, **5**(1), pp. 75-82, 2020.

[9] Gao, F., Guo, W., Song, Q. & Du, F., *Current Development of Heavy-duty Manufacturing Equipments*, Journal of Mechanical Engineering, **46**(10), pp. 92-107, 2010. (In Chinese)

[10] Wang, X., Li, B. & Yang, Z., *Finite Element Analysis and Lightweight Optimization Design on Main Frame Structure of Large Electrostatic Precipitator*, Advances in Materials Science and Engineering, **2018**, pp. 4959632, 2018.

[11] Bendsøe, M.P. & Sigmund, O., *Topology Optimization: Theory, Methods and Applications*. Springer-Verlag Berlin Heidelberg, 2004.
[12] Rozvany, G.I.N., *A Critical Review of Established Methods of Structural Topology Optimization*, Structural and Multidisciplinary Optimization, **37**(3), pp. 217-237, 2009.
[13] Wang, J., Li, Y., Hu, G. & Yang, M., *Lightweight Research in Engineering: A Review*, Applied Sciences, **9**(24), 5322, 2019.
[14] Tyflopoulos, E. & Steinert, M., *Topology and Parametric Optimization-Based Design Processes for Lightweight Structures*, Applied Sciences, **10**(13), 4496, 2020.
[15] Lógó, J., Balogh, B. & Pintér, E., *Topology Optimization Considering Multiple Loading*, Computers & Structures, **207**, pp. 233-244, 2018.
[16] Díaz, A.R. & Bendsøe, M.P., *Shape Optimization of Structures for Multiple Loading Conditions Using a Homogenization Method*, Structural Optimization, **4**, pp. 17-22, 1992.
[17] Allaire, G., Belhachmi, Z. & Jouve, F., *The Homogenization Method for Topology and Shape Optimization, Single and Multiple Loads Case*, Revue Européenne des Éléments Finis, **5**(5-6), pp. 649-672, 1996.
[18] Krog, L.A. & Olhoff, N., *Optimum Topology and Reinforcement Design of Disk and Plate Structures with Multiple Stiffness and Eigenfrequency Objectives*, Computers & Structures, **72**(4-5), pp. 535-563, 1999.
[19] Allaire, G. & Jouve, F., *A Level-set Method for Vibration and Multiple Loads Structural Optimization*, Computer Methods in Applied Mechanics and Engineering, **194**(30-33), pp. 3269-3290, 2005.
[20] Luo, Z., Chen, L-P., Yang, J. & Zhang, Y-Q., *Multiple Stiffness Topology Optimizations of Continuum Structures*, The International Journal of Advanced Manufacturing Technology, **30**(3-4), pp. 203-214, 2006.
[21] Li, H., Gao, L. & Li, P., *Topology Optimization of Structures under Multiple Loading Cases with a New Compliance–Volume Product*, Engineering Optimization, **46**(6), pp. 725-744, 2013.
[22] Qiao, J., Liu, Y., Xu, F., Wu, K. & Zhang, S., *Multi-objective Topological Optimization of an Electric Truck Frame Based on Orthogonal Design and Analytic Hierarchy Process*, IEEE Access, **8**, pp. 140923-140935, 2020.
[23] Cai, K., Shi, J. & Zhang, A., *Stiffness Design of a Continuum under Ill-load Cases by Fractional-Norm Objective Formulation*, Optimization and Engineering, **15**(4), pp. 927-944, 2014.
[24] Li, Y., Yang, Q., Chang, T., Qin, T. & Wu, F., *Multi-load Cases Topological Optimization by Weighted Sum Method based on Load Case Severity Degree and Ideality*, Advances in Mechanical Engineering, **12**(8), pp. 1-15, 2020.
[25] Luo, Z., Chen, L.-P., Yang, J., Zhang, Y-Q. & Abdel-Malek, K., *Fuzzy Tolerance Multilevel Approach for Structural Topology Optimization*, Computers & Structures, **84**(3-4), pp. 127-140, 2006.

[26] Luo, Z., Chen, L., Yang, J., Zhang, Y. & Abdel-Malek, K., *Compliant Mechanism Design Using Multi-Objective Topology Optimization Scheme of Continuum Structures*, Structural and Multidisciplinary Optimization, **30**(2), pp. 142-154, 2005.

[27] Sui, Y., Peng, X., Feng, J. & Ye, H., *Independent Continuous and Mapping Method of Structural Topology Optimization Based on Global Stress Approach*, Frontiers of Mechanical Engineering in China, **5**(2), pp. 130-142, 2010.

[28] Sui, Y.K., Peng, X.R., Feng, J.L. & Ye, H.L., *Topology Optimization of Structure with Global Stress Constraints by Independent Continuum Map Method*, International Journal of Computational Methods, **3**(3), pp. 295-319, 2006.

[29] Young, V., Querin, O.M., Steven, G.P. & Xie, Y.M., *3D and Multiple Load Case Bi-directional Evolutionary Structural Optimization (BESO)*, Structural Optimization, **18**, pp. 183-192, 1999.

[30] Kunakote, T. & Bureerat, S., *Multi-objective Topology Optimization using Evolutionary Algorithms*, Engineering Optimization, **43**(5), pp. 541-557, 2011.

[31] Sun, G., Zhang, H., Fang, J., Li, G. & Li, Q., *Multi-objective and Multi-case Reliability-based Design Optimization for Tailor Rolled Blank (TRB) Structures*, Structural and Multidisciplinary Optimization, **55**(5), pp. 1899-1916, 2017.

[32] Yi, G. & Sui, Y., *TIMP Method for Topology Optimization of Plate Structures with Displacement Constraints under Multiple Loading Cases*, Structural and Multidisciplinary Optimization, **53**(6), pp. 1185-1196, 2016.

[33] Sigmund, O., *A 99 Line Topology Optimization Code Written in Matlab*, Structural and Multidisciplinary Optimization, **21**, pp. 120-127, 2001.

[34] Bendsøe, M.P. & Sigmund, O., *Material Interpolation Schemes in Topology Optimization*, Archive of Applied Mechanics, **69**, pp. 635-654, 1999.

[35] Bendsøe, M.P., *Optimal Shape Design as a Material Distribution Problem*, Structural Optimization, **1**(4), pp. 193-202, 1989.

[36] Marck, G., Nemer, M., Harion, J-L., Russeil, S. & Bougeard, D., *Topology Optimization Using the SIMP Method for Multiobjective Conductive Problems*, Numerical Heat Transfer, Part B: Fundamentals, **61**(6), pp. 439-470, 2012.

[37] McKee, H.J. & Porter, J.G., *Lessons Learned in Part Design from Topology Optimization through Qualification*, in Science in the Age of Experience, Chicago, Illinois, USA, Dassault Systèmes, pp. 54-70, 2017.

[38] Marler, R.T. & Arora, J.S., *Survey of Multi-objective Optimization Methods for Engineering*, Structural and Multidisciplinary Optimization, **26**(6), pp. 369-395, 2004.

[39] Marler, R.T. & Arora, J.S., *The Weighted Sum Method for Multi-objective Optimization: New Insights*, Structural and Multidisciplinary Optimization, **41**(6), pp. 853-862, 2010.
[40] Shi, J. & Gao, Z., *Ill-loaded Layout Optimization of Bi-modulus Material*, Finite Elements in Analysis and Design, **95**, pp. 51-61, 2015.
[41] Cai, K., Gao, Z. & Shi, J., *Compliance Optimization of a Continuum with Bimodulus Material under Multiple Load Cases*, Computer-Aided Design, **45**(2), pp. 195-203, 2013.
[42] Cai, K., Cao, J., Shi, J. & Qin, Q.H., *Layout Optimization of Ill-Loaded Multiphase Bi-Modulus Materials*, International Journal of Applied Mechanics, **08**(03), pp. 1650038, 2016.
[43] Wu, F., Wang, Z., Han, J. & Pei, G., *Research on Multiobjective Topology Optimization of Diesel Engine Cylinder Block Based on Analytic Hierarchy Process*, Mathematical Problems in Engineering, **2019**, pp. 1-16, 2019.
[44] Li, Z. & Wang, M., *Research on Topology Optimization Design for Continuum Structures with Multiple Load Cases*, Modern Manufacturing Engineering, **9**, pp. 70-73, 2008.
[45] Luo, Z., Yang, J., Chen, L-P., Zhang, Y-Q. & Abdel-Malek, K., *A New Hybrid Fuzzy-goal Programming Scheme for Multi-objective Topological Optimization of Static and Dynamic Structures under Multiple Loading Conditions*, Structural and Multidisciplinary Optimization, **31**, pp. 26-39, 2006.
[46] Suresh, K., Ramani, A. & Kaushik, A., *An Adaptive Weighting Strategy for Multi-load Topology Optimization*, presented at the ASME 2012 International Design Engineering Technical Conferences and Computers and Information in Engineering Conference, Chicago, Illinois, USA, 2012.
[47] Ismail, A.Y., Na, G. & Koo, B., *Topology and Response Surface Optimization of a Bicycle Crank Arm with Multiple Load Cases*, Applied Sciences, **10**(6), pp. 1-22, 2020.
[48] Luo, Z., Yang, J. & Chen, L., *A New Procedure for Aerodynamic Missile Designs Using Topological Optimization Approach of Continuum Structures*, Aerospace Science and Technology, **10**(5), pp. 364-373, 2006.
[49] Wang, S., Hou, L., Lee, J. & Bu, X., *Evaluating Wheel Loader Operating Conditions Based on Radar Chart*, Automation in Construction, **84**, pp. 42-49, 2017.
[50] Yildiz, A.R. & Saitou, K., *Topology Synthesis of Multicomponent Structural Assemblies in Continuum Domains*, Journal of Mechanical Design, **133**(1), 011008, 2011.